NUMERICAL SIMULATION OF JET FORMATION BY SHAPED CHARGE AND ITS PENETRATION INTO BUMPERED TARGET

Masahide KATAYAMA*, Atsushi TAKEBA*, Susumu TODA† and Seishiro KIBE†

*Structural Engineering Department, CRC Research Institute, Inc.
2-7-5, Minamisuna, Koto-ku, Tokyo 136, Japan
†National Aerospace Laboratory,
7-44-1 Jindaiji Higashi-machi, Chofu-shi, Tokyo 182, Japan

ABSTRACT

For the purpose of the protection assessment of orbital space debris impacts on the spacecraft, a series of hypervelocity impact tests were conducted by using a shaped charge equipment with the inhibitor in National Aerospace Laboratory of Japan (Ref. 1), which can accelerate an aluminum liner up to approximately 11 km/s jet. The experimental conditions were simulated by a numerical simulation method and both results indicate fairly good agreements. Especially, the numerical simulation made clear the effect of inhibitor on the initial jet formation process, at the same time enabled us to know the physical phase in which the created jet is. And it was proved that multiple-material Eulerian method is applicable not only to the shaped charge jet formation process but also to the successive impact problem of the jet on the target in a single calculational model.

1. INTRODUCTION

A cylinder of chemical high explosive (CHE) with a hollow cavity in one end and a detonator at the opposite end is used in order to obtain hypervelocity metal jet up to approximately 12 km/s. The hollow cavity of conical shape, called "liner", causes the gaseous products formed from the initiation of the explosive at the end of the cylinder opposite the hollow cavity to focus the energy of the detonation products. This acceleration method is referred to "shaped charge", and its phenomenon is known as the Munroe effect mainly in US and UK, while Neumann or Foerster effect in the other countries. A conceptual figure is shown in Fig.1, though there exists an inhibitor in this figure. At present, as are available no experimental methods which can accelerate a solid projectile with the order of 1 gram mass up to above 10 km/s in the laboratory on the ground, the shaped charge is the most effective method to simulate experimentally the orbital space debris impact against the spacecraft in low earth orbit (LEO).

For the purpose of numerical simulation of Munroe effect, some hydrocodes were utilized by using several numerical modeling. In the case of "self-forging-fragment" analyses, of which liner angle is fairly greater than the shaped charge, since the liner material is not subjected to much serious deformations, conventional Lagrangian hydrocodes (Ref. 2) enable us to make numerical simulations up to advanced time stage. On the other hand, in the case of shaped charge analyses it is indispensable to adopt some special numerical methods in order to cope with complicated liner deformations. As an analytical theory of jet formation (Ref. 3) is known to be effective which estimates the jet and slug masses and velocities as functions of the liner collapse velocity and the liner angle at the axis, it is sufficient to calculate the liner collapse velocities from the engineering viewpoint of jet formation analysis. Another is the direct solution method by using Lagrangian rezoning technique applied to complicated liner deformations (Ref. 4), although it is the method overburdening researchers.

It has rarely attempted to solve the overall formation process of shaped charge jet by using Eulerian method, because the thickness of liner is too thin to solve with enough numerical mesh. However, as the computer memory and CPU performance have remarkably improved in recent years, we tried to apply the Eulerian method to liner material. That is, the multiple material Eulerian processor was used to solve all the materials: liner, chemical high explosives, targets, etc. And we

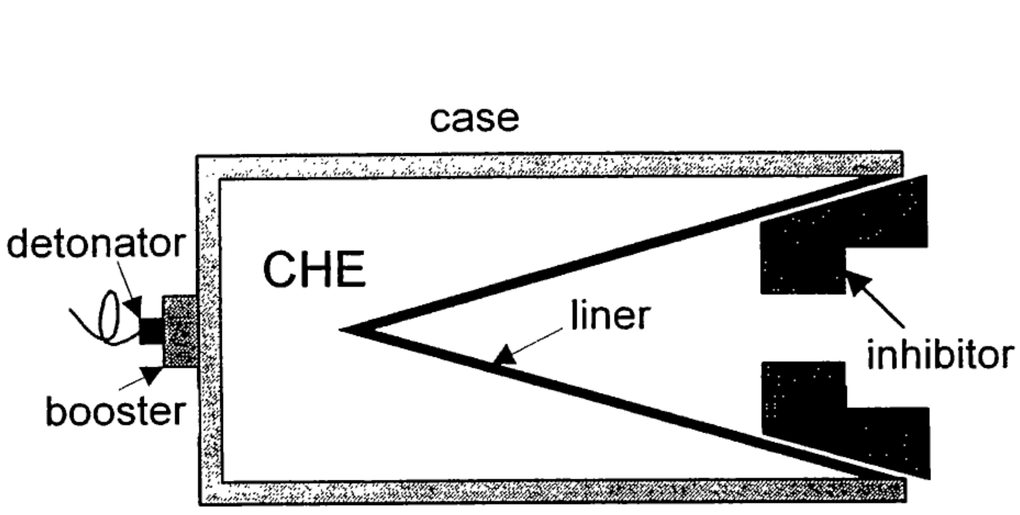

Fig.1 The nomenclature for a conical shaped charge configuration.

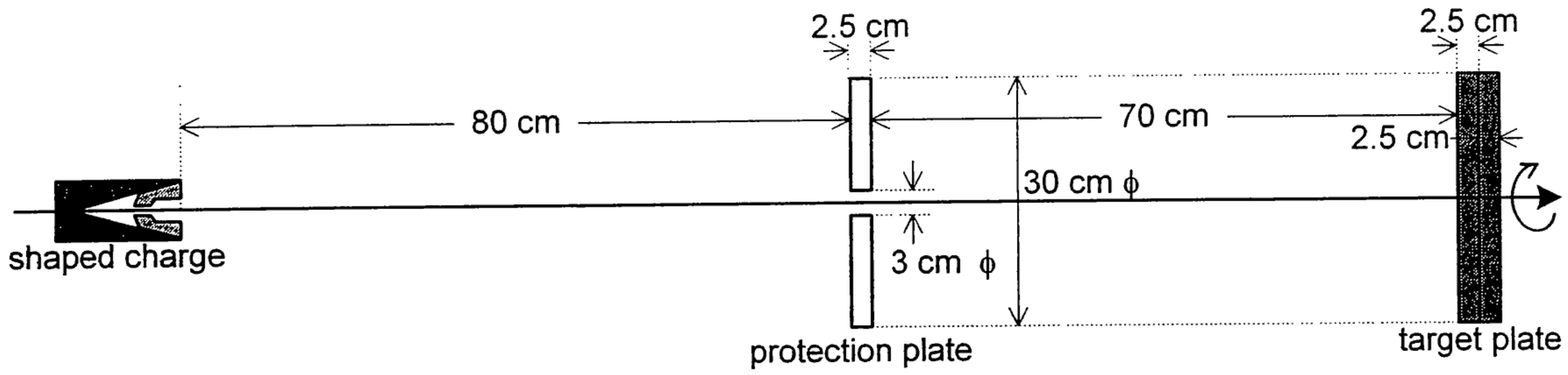

Fig.2 Schematics of the anlytical model to simulate the experimental condition.

obtained the maximum jet velocity of approximately 12 km/s for the aluminum liner. We can see the distribution visually of various field variables in the jet and slug formed from the liner: contour plots of velocity, temperature, density, energy, phase status, etc.

2. NUMERICAL MODELING

Fig. 2 indicates the whole calculational system to simulate the reference experiment. The protection plate was applied in order to trap the inhibitor, liner slug and the blast of the products generated by the detonation of the chemical high explosive. The protection plate is as not to model the Whipple bumper, but this plate has the equivalent meaning of the bumper from the physical viewpoint. The chemical high explosive is OCTOL, the liner is aluminum, protector and two target plates are steel. The protection plate and target plats are 2.5 cm thick.

Two-dimensional hydrocode: AUTODYN-2D™ was applied for the numerical simulation. All the calculations were made in the axisymmetric model. Though this hydrocode is a fully coupled computer program, only the multiple-material Eulerian processor was utilized all the time in this study. The case and inhibitor of the shaped charge were assumed to be perfectly rigid, because their deformations are thought not to be dominant factors in this problem, especially from the viewpoint of the tip jet formation process.

We applied JWL equation of state (E.O.S.) to OCTOL proposed by E. L. Lee (Ref. 5), and using 'on-time burning' model. The equation of the state and its properties are shown in Eq. (1) and Table 1.

$$P = A_{JWL}\left(1-\frac{\omega\eta}{R_1}\right)\exp\left(-\frac{R_1}{\eta}\right) + B_{JWL}\left(1-\frac{\omega\eta}{R_2}\right)\exp\left(-\frac{R_2}{\eta}\right) + \omega\eta\rho_{ref}e, \quad (1)$$

where P is the pressure, η is ρ/ρ_{ref}, ρ is the current density, ρ_{ref} is the reference density, e is the specific internal energy, A_{JWL}, B_{JWL}, R_1, R_2, ω are the material properties

Table 1 Material properties of OCTOL.

variables	properties	(unit)
ρ_{ref}	1.821	(g/cm^3)
A_{JWL}	7.486	(M bar)
B_{JWL}	1.338 x10^{-1}	(M bar)
R_1	4.5	(—)
R_2	1.2	(—)
ω	3.80 x10^{-1}	(—)
V_{det}	8.48 x10^{-1}	(cm/μs)
e_0	9.60 x10^{-2}	(T erg/cm^3)

1 M bar = 10^{11} Pa, 1 T erg = 10^5 J

of the chemical high explosive. And the variables denoted as V_{det} and e_0 in the table are the detonation velocity and the initial internal energy of the high explosive. The constitutive model of OCTOL is assumed to be hydrodynamic.

For the aluminum liner Tillotson equation of state (Ref. 6) and Johnson-Cook constitutive model (Ref. 7) were applied, because the liner is subjected to severe condition. Tillotson E.O.S. can take account of shock-induced vaporization. This E.O.S. is equivalent to Mie-Grüneisen type shock-Hugoniot E.O.S. in the lower pressure region (below 1 T Pa order), and adopts Thomas-Fermi's semi-classic quantum statistic theory in the high pressure region. Tillotson E.O.S. is divided into the following four regions according to the compression μ (ρ/ρ_0-1) and the internal energy E.

I) In the region 1 (if $\mu \geq 0$), the pressure is calculated by Eq. (2).

$$P_1 = \left(a_{Til} + \frac{b_{Til}}{1+\frac{E}{E_0\eta^2}}\right)\eta\rho_{ref}E + A_{Til}\mu + B_{Til}\mu^2 \quad (2)$$

II) In the region 2 (if $\mu < 0$, $E \leq E_s$), the pressure (P_2) is calculated by the equation substituted B_{Til}=0 to Eq. (2).

Table 2 Material properties of aluminum.

	variables	properties	(unit)
E.	ρ_{ref}	2.70	(g/cm^3)
	A_{Til}	7.52 x10^{-1}	(M bar)
	B_{Til}	6.50 x10^{-1}	(M bar)
	a_{Til}	5.00 x10^{-1}	(—)
	b_{Til}	1.63	(—)
O.	α	5.00	(—)
	β	5.00	(—)
S.	E_0	5.00 x10^{-2}	(T erg/g)
	E_s	3.00 x10^{-2}	(T erg/g)
	E_s'	1.50 x10^{-1}	(T erg/g)
C.	G	2.76 x10^{-1}	(M bar)
	A_{J-C}	2.65 x10^{-3}	(M bar)
	B_{J-C}	4.26 x10^{-3}	(M bar)
	C_{J-C}	1.50 x10^{-2}	(—)
M.	m	1.00	(—)
	n	3.4 x10^{-1}	(—)
	T_{melt}	7.75 x10^2	(K)
	C_{cv}	8.75 x10^{-6}	(T erg/g K)

E.O.S.: equation of state, C.M.: constitutive model, G: shear modulus, C_{cv}: constant volume specific heat, 1 M bar = 10^{11} Pa, 1 T erg = 10^5 J

Ⅲ) In the region 3 ($\mu < 0$, $E_s < E < E_s'$), the pressure is calculated by Eq. (3).

$$P_3 = P_2 + (P_4 - P_2)(E - E_s)/(E_s' - E_s) \qquad (3)$$

Ⅳ) In the region 4 ($\mu < 0$, $E \geq E_s'$), the pressure is calculated by Eq. (4)

$$P_4 = a_{Til}\eta\rho_{ref}E + \left[\frac{b_{Til}\eta\rho_{ref}E}{1+\frac{E}{E_0\eta^2}} + A_{Til}\mu\right] \times \exp\left\{\beta\left(1-\frac{1}{\eta}\right)\right\} \exp\left\{-\alpha\left(1-\frac{1}{\eta}\right)^2\right\} \qquad (4)$$

where E is the current specific internal energy (energy per unit mass), E_s and E_s' is the specific internal energy with relation to the sublimation point. E_0 is the specific internal energy at 0℃. The variables indicated by a_{Til}, b_{Til}, A_{Til}, B_{Til}, α, β are the properties characteristic of the material.

In the Johnson-Cook constitutive model applied to the aluminum liner the yield stress (Y) is estimated by the function of strain (ε), strain rate ($\dot{\varepsilon}$) and homologous temperature (T*) by Eq. (5).

$$Y = (A_{J-C} + B_{J-C}\varepsilon^n)(1 + C_{J-C}\, ln\,\dot{\varepsilon})(1 - T^{*m}), \qquad (5)$$

where $T^* = (T - T_{room})/(T_{melt} - T_{room})$ (6)

and T_{room} and T_{melt} are the room temperature and melting temperature, respectively. A_{J-C}, B_{J-C}, C_{J-C}, m and n are the properties characteristic of the material. And as a fracture condition we used the value of spall strength (negative maximum hydrostatic pressure) of 0.0 Pa, not as to affect the expansion after the liner becomes hydrodynamic.

Equally, Tillotson E.O.S. and the Johnson-Cook constitutive model were applied to the steel protection plate and steel targets. The material properties for them are shown in Table 3. As fracture conditions both the spall strength and the ultimate strain were applied to them by which the numerical cell is triggered to be fractured instantaneously. The value of spall strength used in the calculation is −2.0 GPa and that of the ultimate strain is 25 %.

3. RESULTS OF NUMERICAL ANALYSES AND COMPARISON WITH THE EXPERIMENT

Fig. 3 indicates the early stages of aluminum jet formation processes, in order to comprehend the effect of inhibitor. The figures in the left-hand side are material fraction plots of aluminum materials. In the case modeling the inhibitor, the tip of jet is hollow but separated

Table 3 Material properties of the steel of protection plate and target plates.

	variables	properties	(unit)
E.	ρ_{ref}	7.86	(g/cm^3)
	A_{Til}	1.279	(M bar)
	B_{Til}	1.05	(M bar)
	a_{Til}	5.00 x10^{-1}	(—)
O.	b_{Til}	1.63	(—)
	α	5.00	(—)
S.	β	5.00	(—)
	E_0	9.50 x10^{-2}	(T erg/g)
	E_s	2.44 x10^{-2}	(T erg/g)
	E_s'	1.02 x10^{-1}	(T erg/g)
C.	G	8.18 x10^{-1}	(M bar)
	A_{J-C}	3.50 x10^{-3}	(M bar)
	B_{J-C}	2.75 x10^{-3}	(M bar)
	C_{J-C}	2.20 x10^{-2}	(—)
M.	m	1.00	(—)
	n	3.6 x10^{-1}	(—)
	T_{melt}	1.81 x10^3	(K)
	C_{cv}	4.52 x10^{-6}	(T erg/g K)

E.O.S.: equation of state, C.M.: constitutive model, G: shear modulus, C_{cv}: constant volume specific heat, 1 M bar = 10^{11} Pa, 1 T erg = 10^5 J

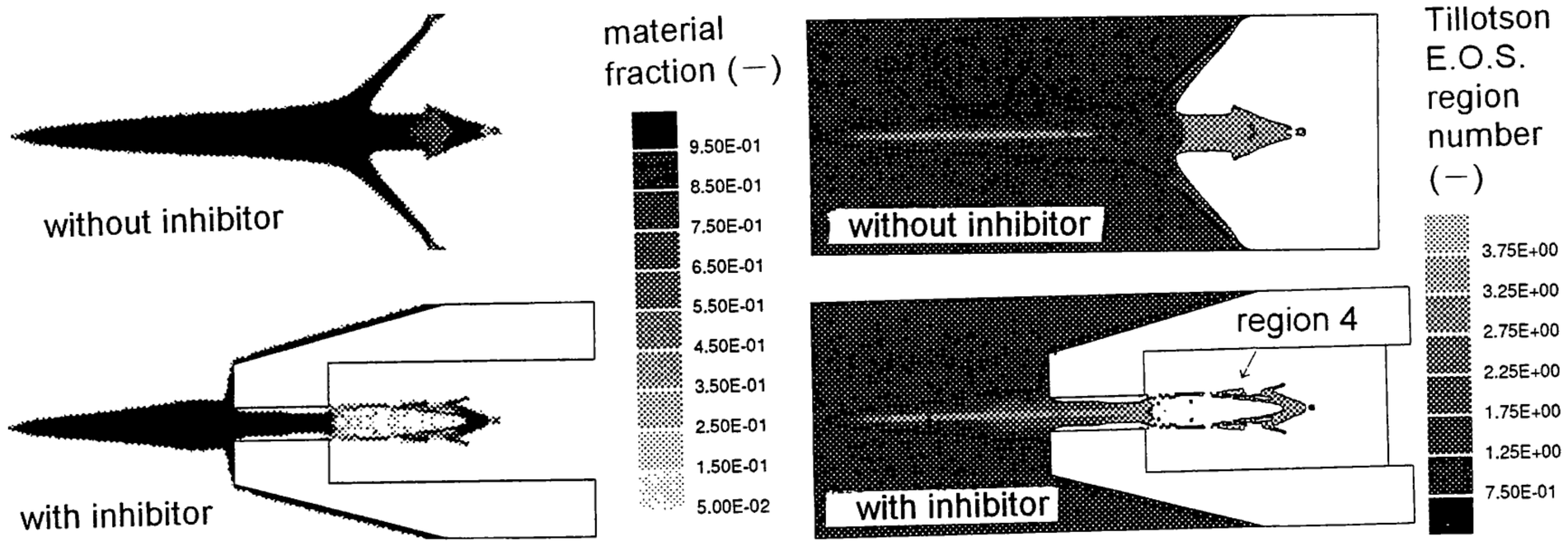

Fig.3 The comparison of the material fraction and Tillotson's region number contour plots at 20 μs.

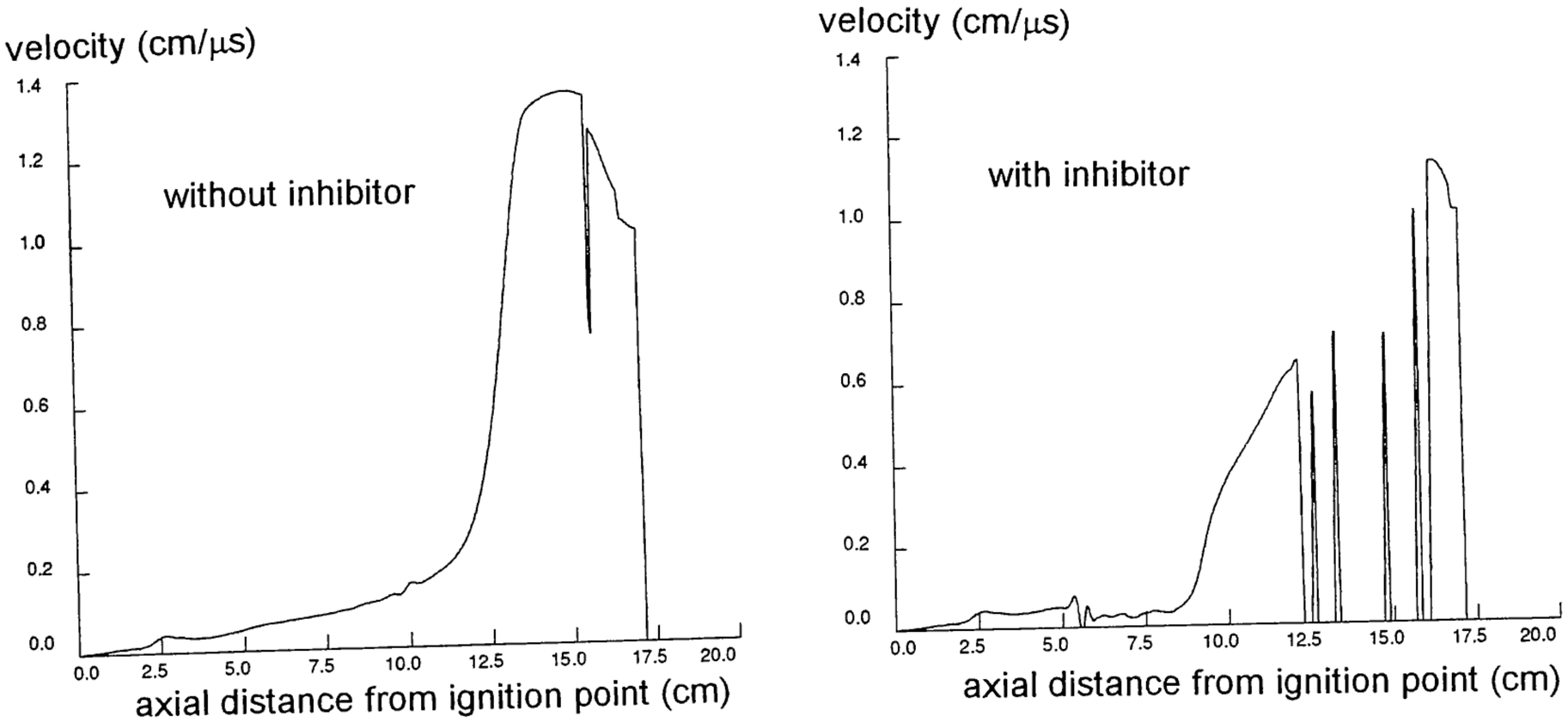

Fig.4 Profile plots of the axial jet velocity along the axis at 20 μs.

from the aluminum slug efficiently. The fact is ascertained experimentally that the conical shaped charge using inhibitor forms the hollow jet. The figures in the right-hand side show the contour plots of the region number mentioned in the description about Tillotson E.O.S. In the case modeling the inhibitor, a portion of region 4 (completely vaporized phase) is estimated in the lateral part of the jet tip, while other light colored regions are corresponding to region 3 (solid-vapor-multiphase) in both cases. The region number for CHE has no meanings in these plots. Fig. 4 indicates the comparison of the profiles of axial jet velocities along the center of symmetrical axis. In the case modeling inhibitor maximum jet velocity is lower than another one, and the hollow effect also appears in this graph, since this graph is plotted along the axis. However, the jet tip of the case modeling inhibitor is broader than another one.

Fig. 5 depicts the overall phenomena of the jet formation and its impact on the multiple targets in the case of conical shaped charge with the inhibitor. The calculated profile of the jet tip at 40 μs is similar to the experimental result, although it should be noted that two figures have a difference between three-dimensional projection and two-dimensional slice plots in themselves. We can see visually the process of jet's expanding and impacting on the target plates from the velocity distribution plots at 50 through 250 μs in Fig.5. Consequently the jet forms a crater with a depth (2.5 cm) just same as front target thickness from the material distribution profile at 250 μs in Fig. 5. The average depth of the target crater obtained by experimental ten shots is 2.42 cm, the calculational result has a fairly good agreement with experimental result. These results were obtained by using the Eulerian rezoning technique, that is, deleting backward numerical meshes when they are no longer required to be included in the calculational system and

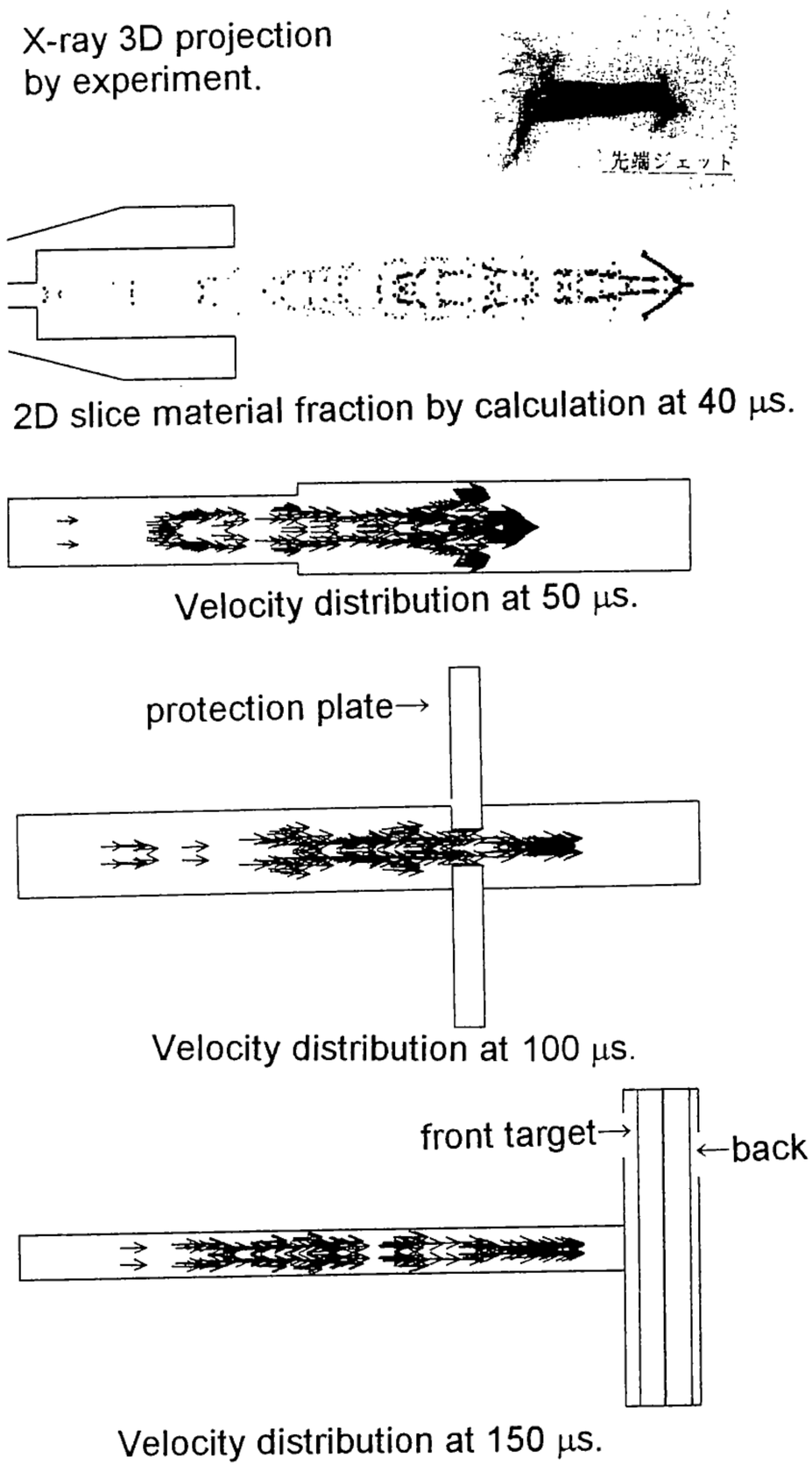

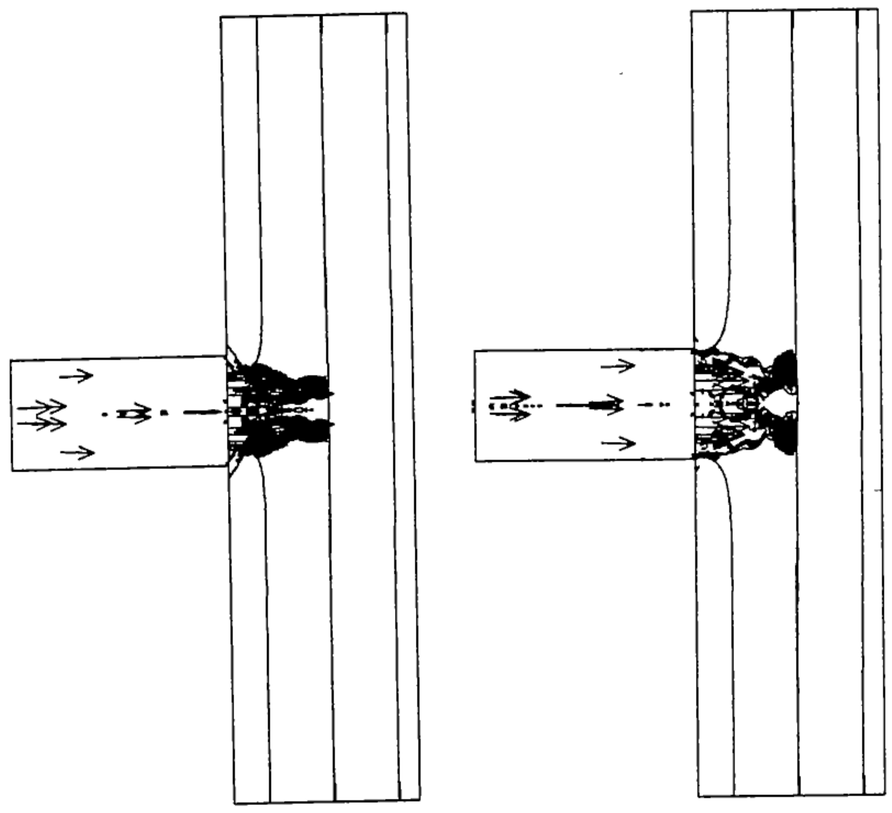

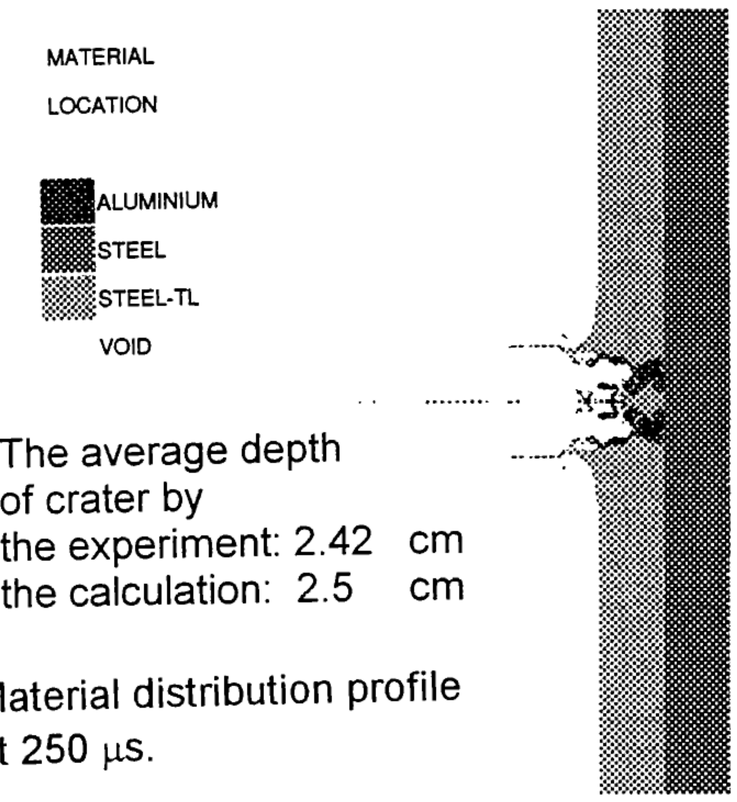

Fig. 5 The visualized summary of comparison between calculation and experiment.

adding new Eulerian meshes forward gradually. This method does not burden us so much, as compared with the Lagrangian rezoning method. We carried out about 10 times Eulerian rezoning procedures to accomplish the whole calculation, but we can do that for a couple of days by using any current typical engineering workstation or Pentium® Pro PC.

4. CONCLUDING REMARKS

1) The calculated jet velocity, jet profile and target crater created by the conical shaped charge with the inhibitor were compared successfully with those of experimental results. The multiple-material Eulerian method is proved to be sufficiently applicable to such a big scale and/or long term problem as hypervelocity impact phenomena.

2) The effect upon the jet formation process in the conical shaped charge accelerator with the inhibitor was made clear and demonstrates visually at the early stage through the present numerical analyses.

3) The physical phase of the jet created by the shaped charge was made clear through the present numerical analyses, probably at the first time in the world, provided that the liner material would be subject to Tillotson E.O.S.

4) Since one of the authors has already ascertained that the multiple-material Eulerian method is appli-

cable to the hypervelocity (6－14 km/s) impact problem against the stuffed Whipple bumper shield (Ref. 8), the numerical analysis of the shaped charge jet impact against the stuffed Whipple bumper shield will be able to be performed in the similar procedures.

However, the Eulerian solution scheme is a diffusive numerical method in itself, mainly because of the necessity of the convection calculation procedure. It will be important and realistic to adopt some higher order solution scheme in near future judging from the recent remarkable progress of the computer hardware, although we make use of the double precision calculation in the present numerical analyses.

5. REFERENCES

1. S. Toda, S.Kibe, T. Yamamoto, M. Kobayashi, A. Kunoh, H. Miyoshi and M. Hikiji, "Study of Hypervelocity Impact Testing with Shaped Charge (Part2)," *Proc. Symposium on Shock Wave*, Japan Society of Shock Wave Research, 1996 (in Japanese).

2. R. G. Whirley and B. E. Engelmann, "DYNA2D A Nonlinear, Explicit, Two-Dimensional Finite Element Code For Solid Mechanics User Manual," *UCRL-MA-110630*, LLNL, 1992.

3. E. M. Pugh, R. J. Eichelberger and N. Rostoker, "Theory of Jet Formation by Charges with Lined Conical Cavities," *J. App. Phys.*, Vol.23 No.5, 1952.

4. S. Hancock, H. Hancock and L. Behrmann, "Full Lagrange and Lagrange-Euler Shaped Charge Jetting Calculation," *PIIR-3-82*, Physics International Company, 1982.

5. E. L. Lee, F. H. Helm, M. Finger and J. R. Walton, "Equations of state for Detonation Products of High Energy PBX Explosives," *UCID－17540*, LLL, 1977

6. J. H. Tillotson, "Metallic Equations of State for Hypervelocity Impact," *GA-3216*, General Atomic, 1962

7. G. R. Johnson and W. H. Cook, "A Constitutive Model and Data for Metals Subjected to Large Strains, High Strain Rates and High Temperatures," *Proc. 7th Int. Symp. On Ballistics*, The Hague, 1983

8. K. Shiraki, M. Harada, S. Terada and M. Katayama, "Hydrocode Simulation for Space Debris Impact," *Proc. of the 40th Space Sciences and Technology Conference*, 1996 (in Japanese).